Send Orders of Reprints at reprints@benthamscience.org

50 *The Open Construction and Building Technology Journal,* 2012, *6,* (Suppl 1-M3) 50-62

Open Access

Rotations of RC Members of Infilled Frames at Yielding and Ultimate

D.J. Kakaletsis*

Reinforced Concrete Laboratory, Technological Educational Institution of Serres, 62124 Serres, Greece

Abstract: The influence of masonry infills with openings on the rotations of RC members of infilled frames at yielding and ultimate under seismic loading is investigated. Fifteen 1/3-scale, single-story, single-bay frame specimens were tested under reversed cyclic, quasi-static, horizontal loading up to a drift level of 40‰. The parameters investigated include the shape, the size, the location of the opening and the infill compressive strength. Relative hinge rotation at the ends of the beams and columns were calculated by a pair of displacement transducers placed on the surface of the frame members. Based on the load against rotation envelope curves of each cross-section**,** the deformation at yielding, θ_y, and the ultimate deformation capacity, θ_u, corresponding to a lateral force response equal to 85% of the maximum, were measured and compared with the values given by FEMA reports. Consequently, a reduction factor is proposed for FEMA values.

Keywords: Experiments, infilled frames, infill openings, rotations of R/C members.

INTRODUCTION

The inelastic deformation capacity of reinforced concrete (RC) members is important for the resistance of RC structures to imposed deformation from seismic loads because earthquake-resistant design relies on ductility, that is, on the ability of RC members to develop deformations well beyond elastic limits without significant loss of load-carrying capacity. Due to the emergence of displacement-based concepts for seismic design of new structures and seismic evaluation of old ones, quantification of deformation capacity in terms of geometric and mechanical characteristics of members and of their reinforcement have attracted increased interest in recent years. The first new-generation guidelines for seismic rehabilitation of existing buildings (ATC 1997) [1, 2] adopted nonlinear static analysis (commonly called "push-over" analysis) as the reference method for assessment of existing or retrofitted buildings, or for evaluation of the seismic performance of new designs. Since then, its appealing simplicity and intuitiveness and the wide availability of reliable and user-friendly analysis software have made it the analysis method of choice for seismic assessment and retrofitting of buildings. The 1997 NEHRP Guidelines for the seismic rehabilitation of Buildings [1, 2] base member evaluation on a capacity-demand comparison in terms of member deformations. These guidelines, known as FEMA 273/274 [1, 2] and more recently FEMA 356 [3] as well as other current procedures for the analysis of the seismic response, in reference [4], require realistic values of the effective cracked stiffness of RC members for reliable estimation of the seismic force and deformation demands. To this end, tools are needed for the calculation of the secant stiffness to yielding for known geometric and mechanical characteristics of RC members.

The secant stiffness to yielding and the ultimate deformation of RC members are commonly determined (assuming purely flexural behavior), from section moment-curvature relations and integration thereof along the member length. More advanced models that incorporate the effects of inclined cracking, bone-slip, and tension stiffening, and account for the detailed σ-ε behavior of the reinforcement have also been proposed for the plastic rotation capacity of beams under monotonic loading in references [5, 6]. Despite their sophistication, these models have thus far not been very successful in effectively reproducing the experimental behavior up to ultimate. Test results constitute the ultimate recourse for validation, calibration, or even development of models, as presented in reference [7]. This is particularly true for complex phenomena, such as the deformational behavior of concrete members up to the failure in monotonic or cycling loading.

On the other hand, field experience and analytical and experimental research (Fardis and Panagiotakos 1997, Fardis 2000) [8, 9] have demonstrated that non-structural elements, notably masonry infills, may interfere in the seismic response of RC structures. Indeed, in masonry-infilled structures, the presence of infill walls has overall beneficial effect on seismic performance, especially when the building structure itself has poor engineered earthquake resistance. However, if the contribution of masonry infills to the lateral strength and stiffness of the building is large relative to the strength and stiffness of the structure itself, the infills may override the seismic design of the structure and undermine the efforts of the designer and the intention of design codes to control the inelastic response by spreading the inelastic deformation demands throughout the structure (Fardis 2009) [10]. In addition to this potential detrimental effect of infills on global response, there may also be local adverse effects of infills (Moghadam and Dowling 1987, CEB 1996, FEMA 356, 2000) [3, 11, 12]. Among these, there is the case of stiff and strong infills that may shear – off weak columns, especially for imbalanced (i.e., one – sided) contact. According to the above adverse local effect, failure or heavy damage of an

*Address correspondence to this author at the Reinforced Concrete Laboratory, Technological Educational Institution of Serres, 62124 Serres, Greece; Tel: +30 23210 49257, 49151; Fax: +30 23210 46556;
E-mail: dkak@teiser.gr

infill panel may dislodge part of it, exerting a concentrated force on the adjacent column. The stronger the infill, the larger is the magnitude of this force and the higher the likelihood of column shear failure in spite of the presence of openings, as presented in reference [13]. Nevertheless, experimental results that have been reported by Kakaletsis and Karayannis 2007, 2008, and 2009 [14-16] show the significance of various forms of openings on the reduction of strength, stiffness and energy dissipation capability for the examined cases of infilled frames. The use of infill with improved compressive strength but almost identical shear strength decreases the influence of the openings in terms of resistance, stiffness, ductility and energy dissipation capacity. Based on these results it was deduced that masonry infills with eccentrically located openings has been proven to be beneficial to the seismic capacity of the bare RC frames in terms of strength, stiffness, ductility and energy dissipation.

With this in mind, and considering that tests are the main source of information for the cyclic behavior of concrete members up to failure, the same experimental data were used herein for the determination of the deformations of RC members of infilled frames at yielding and at failure in terms of the geometric and mechanical characteristics for the infill walls. The primary deformation measure considered herein is the drift of chord rotation θ of a member over the shear span. This measure captures the macroscopic behavior of the member as a whole, relates readily to more global measures of seismic response–such as story drifts–while at the same time suffices for signaling failure at the local level.

The determined values for the deformation at yielding and for the ultimate deformation capacity of RC members of infilled frames are essential for the application of displacement-based procedures for earthquake-resistant design of new RC structures and for seismic evaluation of old ones. Currently, publications like FEMA 356 [3] and ATC-40 [4] contain provisions for the capacities of generalized deformation taken as rotation for beams and columns in noninfilled portions of frames, while such provisions are not provided for infilled portions of frames. However, a realistic estimation of the effective elastic stiffness of cracked RC members and structures is important for the calculation of seismic force and deformation demands.

EXPERIMENTAL PROGRAM

Test Specimens

The experimental program as shown in Table **1** and Fig. (**1**) consisted of fifteen tests of single - story one - bay 1/3 - scale specimens of reinforced concrete frames with infills of "weak" clay brick and "strong" vitrified ceramic brick. The program results provide data for the evaluation of the influence of different opening shapes, different opening sizes, different opening locations and different infill compressive strengths on the surrounding frames. The program included the test of: reference frame specimens (bare frame and frame specimens with solid weak and solid strong infills), frame specimens with concentric window and door opening with three sizes, frame specimens with eccentric window and door opening in infills with two eccentricities, frame specimens with concentric window and door opening in weak and strong infills. The complete information and detailed results of the aforementioned experimental study

Table 1. Test Specimens

Specimen Notation	Opening Shape		Opening Size l_a/l				Opening Location x/l			Masonry type	
	Window	Door	0	0.25	0.38	0.50	0.17	0.33	0.50	Weak	Strong
B	Bare	Bare									
S	Solid	Solid	•							•	
WO2	•			•					•	•	
WO3	•				•				•	•	
WO4	•					•			•	•	
DO2		•		•					•	•	
DO3		•			•				•	•	
DO4		•				•			•	•	
WX1	•			•			•			•	
WX2	•			•				•		•	
DX1		•		•			•			•	
DX2		•		•				•		•	
IS	Solid	Solid	•								•
IWO2	•			•					•		•
IDO2		•		•					•		•

l = length of masonry infill, l_a = width of opening, x = distance between opening center – edge of infill.

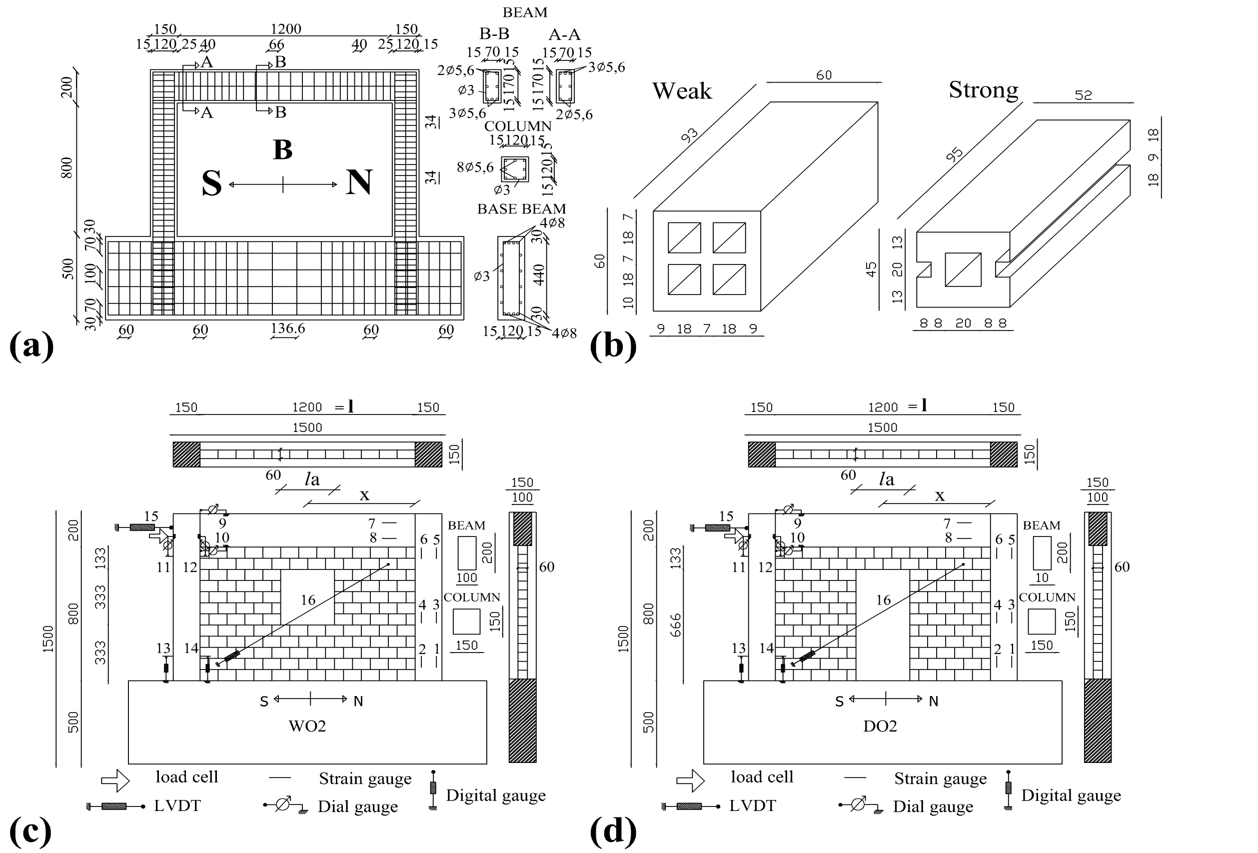

Fig. (1). Description of infilled frame specimens and instrumentation (mm): (**a**) reinforcement detailing of the R/C frame model; (**b**) weak and strong brick units; (**c**) specimen with window opening and instrumentation; (**d**) specimen with door opening and instrumentation.

have been reported in references [14-16].

The geometric characteristics of the RC frames were the same for all specimens. The elevation, the corresponding cross-sections of the members and the design details for the RC frame specimens are shown in Fig. (**1a**). The beam and the column cross sections were 100×200 mm and 150×150 mm respectively. The above dimensions corresponds to one third (1/3) scale of the prototype frame sections, 300×600 mm for the beam and 450×450 mm for the column. The column had closer stirrups throughout the length, because the entire length of columns that are in contact with infills on one side per vertical plane are subjected to the special detailing and confinement requirements applying to critical regions. The beam had more shear reinforcement in the critical regions. Each beam-to-column joint had five horizontal stirrups to prohibit brittle shear failure. The longitudinal reinforcement diameter Φ5.60 mm and stirrups diameter Φ3 mm of the frame members corresponds to one third (1/3) scale of Φ18 mm and Φ8 mm reinforcement diameters respectively of the prototype frame. The transverse reinforcement in the critical regions of specimens satisfied the requirements of the Greek standards, s_h = 34 mm ≈ $s_{h(required)}$ = 33.3 mm for the columns and s_h = 40 mm < $s_{h(required)}$ = 56 mm for the beams and corresponds to one third (1/3) scale of s_h = 100 mm ≈ $s_{h(required)}$ for the columns and s_h = 120 mm < $s_{h(required)}$ = 180 cm for the beams of the prototype frame. At the specimens, low strength plain bars were used, although the rule for the construction practice is to use high strength deformed bars. Although the possible consequences from the use of low strength plain bars, particularly in terms of RC members deformability, are well known, the reasons, for this use, is due to the scale of the specimens and the availability of the scaled diameters in the market. The reinforced concrete frame represented a typical ductile concrete construction, built in accordance with the currently used codes and standards in Greece, which are very similar to Eurocode 8 (CEN 2004) [17]. The average sum of the flexural capacity of column to that of beam was also confirmed by these standards. Thus, for the beam-column connections examined in this investigation, the ratio was 1.50, greater than 1.40. The purpose was to push the formation of plastic hinge in the beams. Masonry infill in the model had a height of 800 mm and a length of 1200 mm, as shown in Figs. **(1c**, **d)**, representing an exterior partition wall of the prototype structure with a height of 2.40 m and a length of 3.60 m (height against length ratio H/L=1/1.50). In the experiments a brick with dimensions 60×60×93 mm was used for the "weak" common clay brick usually used in Greece and obtained by cutting a certain brick with dimensions 60×90×185 mm. The experimental brick unit corresponds to one third (1/3) scale of the prototype brick unit with dimensions 180×180×300 mm, which is used in typical partition walls. On the other hand a brick with dimensions 52×45×95 mm was used for the "strong" vitrified ceramic brick that proved to be important for the specimen behaviour and obtained by cutting an available on the market brick with dimensions 52×45×190 mm. The experimental brick unit corresponds to one third (1/3) scale of the prototype brick unit with dimensions160×140×300 mm. It is obvious that the partition wall was not scaled down very successfully in this case. Brick shape is shown in Fig. (**1b**). A representative mortar mix was used for the two types of infills contained the portions 1:1:6 (cement: lime: sand) and produced mechanical properties similarly to type M1 mortar according to EN 998-2 standard (CEN 2001) [18]. Infills were designed so that the lateral cracking load of the infill is less than the available column shear resistance. Masonry properties, as presented in the following section 2.2, were chosen in such a way to obtain the desired weak masonry lateral strength for both infill types. Cracking shear of infill without the confinement offered by the surrounding frame was:

$$V_{w,u} = f_v \cdot t \cdot l = 27.36 \text{ or } 25.58 \text{ kN} \tag{1}$$

where f_v is the masonry shear strength of the bed joints subjected to normal stress f_n, from diagonal tests on full size bare infills ($f_v/f_n = l/H = 1.5/1$, as shown in Table **2**), l is the length of masonry infill, t is the thickness of masonry infill. It must be pointed out that shear strength of the weak masonry wall is a little higher than the corresponding one of the strong masonry, due to the thickness reduction. Assuming that plastic hinges occurred at the bottom and the top of the columns, flexural resistance of the bare frame was:

$$F_f = 4M_{pc}/h = 42.48 \text{ kN} \tag{2}$$

where M_{pc} is the plastic moment of the column considering the effect of the axial force, $h = H - l_p$, H is the height of masonry infill, l_p is the plastic hinge length equal to 0.5 times the column depth. $V_{w,u}$ was lower than F_f. This closely represents actual construction in Greece.

Material Properties

Material tests were conducted on concrete, reinforcing steel and masonry samples. The mean compressive strength of the frame concrete was 28.51 MPa. The yield stress of longitudinal and transverse steel was 390.47 and 212.2 MPa respectively. The main results of mortar, bricks and infill masonry tests are presented in Table **2**. The relationship of the shear strength of the bed joints f_v versus the normal stress f_n, derived from the cohesion tests and the diagonal compression tests of masonry panels with various length L to height H ratios and full size panels as well ($f_v/f_n = l/H$) is presented in Table **2**. It can be noted from the Table **2** that the compressive strength of the "weak" masonry prisms was lower than that of the "strong" ones while the shear strength of the bed joints in the "weak" and "strong" specimens compared with the same of the full size infills length / height ratio ($l/H = 1.5/1$) were almost identical.

Test Setup and Instrumentation

Since the scope of this study was to compare the frame behavior with reference to masonry infill type, an arbitrarily selected quasi-static reversed cyclic lateral load and an axial compressive load per column were applied. The test setup is shown in Fig. (**2**). The lateral load was applied by means of a double action hydraulic actuator. The vertical loads were exerted by manually controlled hydraulic jacks that were tensioning four strands at the top of the column whose forces were maintained constant during each test. The level of this

Table 2. Mechanical Properties of the Materials Used (MPa)

Material Properties	**Masonry Type**	
	Weak t = 6 cm	**Strong** t = 5.2 cm
MORTAR		
Compressive Strength f_m	1.53	1.75
BRICK UNITS		
Compressive Strength f_{bc}	3.1	26.4
MASONRY		
Compressive Strength ⊥ to hollows f_c	2.63	15.18
Elastic Modulus ⊥ to hollows E	660.66	2837.14
Compressive strength // to hollows f_{c90}	5.11	17.68
Elastic Modulus // to hollows E_{90}	670.3	540.19
Friction Coefficient (without units) μ	0.77	0.957
Shear Modulus G	259.39	351.37
Shear Strength without normal stress f_{vo}	0.08	0.12
Shear Strength with normal stress f_v / f_n †	0.38/0.25*	0.41/0.27*
	0.33/0.22	0.26/0.17
	0.39/0.30	0.60/0.61
	0.21/0.37	0.39/0.72
	0.20/0.73	0.41/1.55

†On masonry panels of length l and height H, $f_v / f_n = l / H$.
*On full size infills l/H = 120 cm / 80 cm.

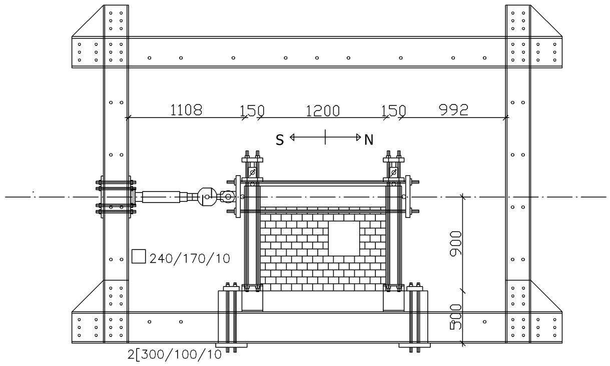

Fig. (2). Test setup (mm).

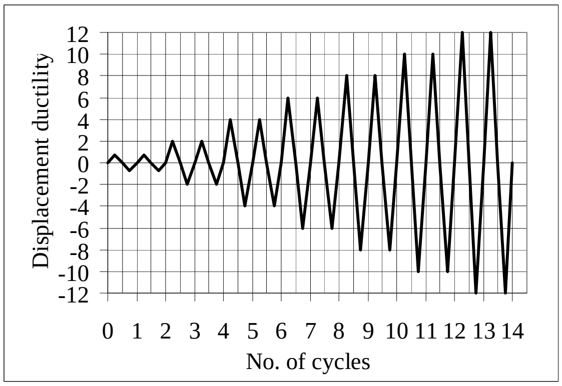

Fig. (3). Loading programme.

axial compressive load per column was set 50 kN (0.1 of the ultimate). The axial force applied to the columns of 50 kN was considered to prevent the columns from developing tension, as shown from the moment-thrust interaction diagram for the columns of the frame. Besides, axial force was dictated by the availability of the formwork and the laboratory testing capacities. One LVDT measured the lateral drift of the frame and a load cell measured the lateral force of the hydraulic actuator. Strain gauges 1 to 8 were placed on the center steel bars of the members at their critical sections, to monitor directly the behavior of the reinforcement steel during tests. The loading program included full reversals of gradually increasing displacements. Two reversals were applied for each displacement level. The cycles started from a ductility level 0.8 corresponding to an amplitude of about ±2 mm (the displacement of yield initiation to the system is considered as ductility level μ=1) and were followed gradually by ductility levels 2, 4, 6, 8, 10, 12 corresponding about to amplitudes 6, 12, 18, 24, 30, 36 mm Fig. (**3**).

Relative joint rotations between the beams and columns were measured by a pair of displacement transducers. Dial gauges 9 to 12, and digital gauges 13 and 14 were placed at critical sections of the frame to estimate the relative rotation of the members, as shown in Figs. **(1c** and **d)**. Due to symmetry, in most specimens, only two of the joints were instrumented – namely the lower and the upper south joints. The positions utilized at the joints for measuring joint rotations were kept the same for all tests, on the end of the plastic hinge length, equal to 0.5 times the member depth. Relative hinge rotation at the ends of the beams and the columns were calculated as illustrated by Fig. (**4**). Some representative compatibility checks were carried out, based on the rotations measured at ends of each member and on the measured lateral drift of the frame. It was derived that the sum of the rotations measured at the top and bottom ends of each column was almost equal to the total column drift where there was no rotation at beam ends.

Test Results

The hysteretic response envelopes of applied lateral force versus the calculated rotations were plotted and are presented at Figs. **(5, 6)** and **(7)**. Normally, the rotations of RC members have to be evaluated on a load rotation curve where the

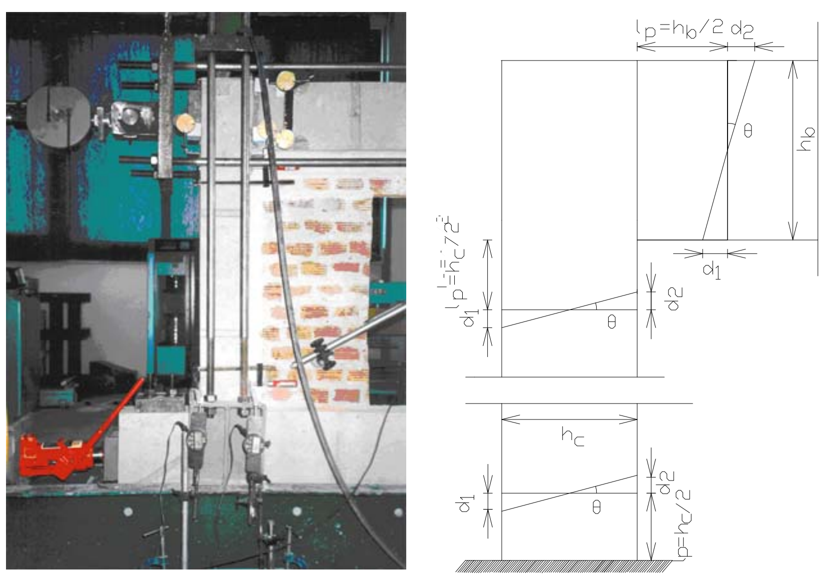

(a) (b)

Fig. (4). (**a**) Locations for displacement transducers. (**b**) Determination of joint rotation $\theta = (d_1+d_2) / h$, where h_c = 150mm for the column and h_b = 200mm for the beam.

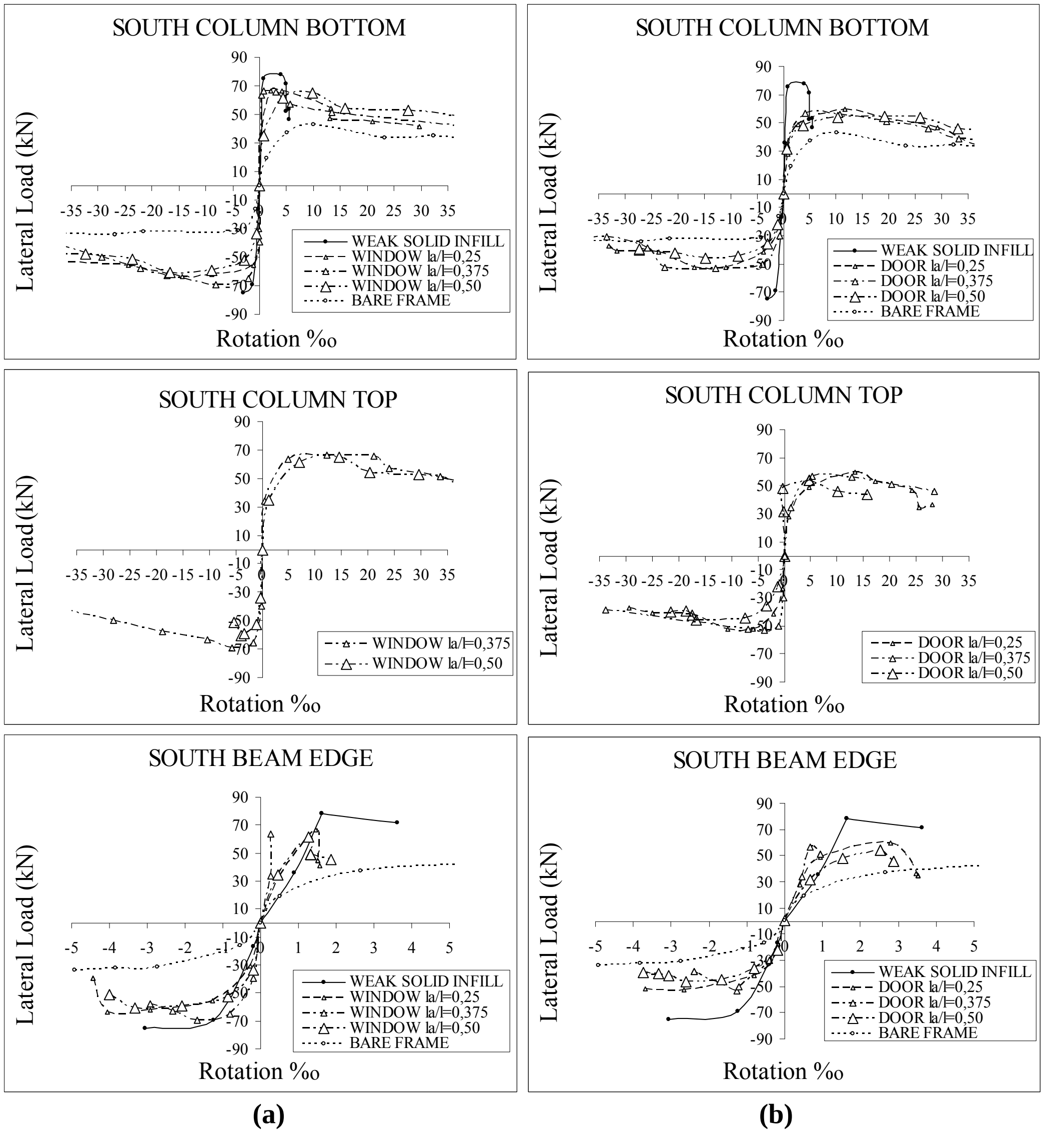

Fig. (5). Lateral load-rotation envelopes: (**a**) window openings of various sizes; and (**b**) door openings of various sizes.

load is the moment applied to the end section of member (or equivalently the lateral load applied to a cantilever member with a given shear span). In this paper the "lateral load" reported in the experimental curves includes the contribution of different RC members and of the infill panel. However, it is assumed that the evaluated load displacement curve is representative of a single RC member's behavior because the frame and the infill are considered as two parallel systems with displacement compatibility at the compression corners, the interaction of this type of the infill and the frame introduces no significant influence on the lateral behavior (the lateral strength is almost equal to the sum of the strengths of the individual components), plastic hinges are assumed to develop at both ends of the columns and no significant shear transfer is assumed between the beam and the infill, as have been reported in Kakaletsis and Karayannis 2008 [15].

Members, detailed for earthquake resistance, normally do not fail abruptly under cyclic loading. Their failure in flexure is typically gradual, governed by the progressive deterioration of the compression zone. Damage starts with spalling of the cover concrete and normally continues with buckling of the bars that lose their lateral support and finally with disintegration of the core concrete. When there are no clear signals of failure, the member may be considered to have failed if, from a certain point on, the pattern of the response changes. For example, when, during constant amplitude cycling the peak force drops disproportionately from one cycle to the next ("strength decay"), compared to previous cycles at the same or smaller deformation amplitude. No matter whether the loss of strength is abrupt or gradual, a conventional definition of member failure under cyclic loading is necessary. A 20% strength decay on the load displacement curve of the RC member is usually assumed as ultimate condition (Fardis 2009) [10]. Yielding rotation if not evaluable based on a section analysis is usually taken at 70-80% of maximum strength (Sezen 2002, Elwood and Eberhard, 2009) [19, 20]. Given that frames did not exhibit a significant load degradation after the maximum load resistance had been reached, a definition covering both the abrupt and the gradual change in the force-deformation response has been

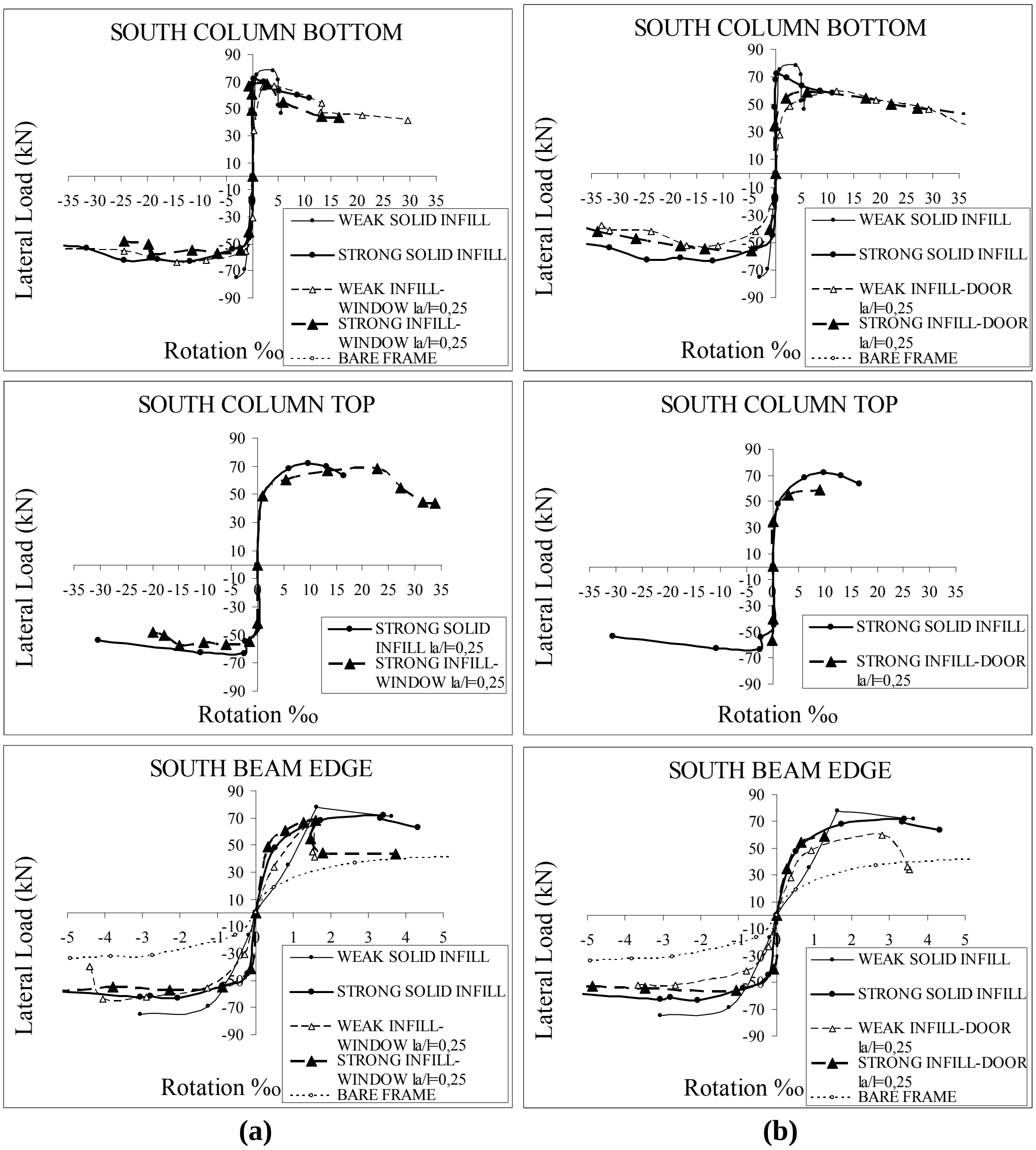

Fig. (6). Lateral load-rotation envelopes: (**a**) weak and strong infill with window; and (**b**) weak and strong infill with door.

proposed in the present study. According to it, failure is taken to occur when it is not possible to increase the force resistance above 85% of the maximum resistance attained during the test, even though the imposed deformation keeps increasing. In the experiments, the conventional identification of failure with a 15%-drop in post-ultimate resistance coincides with a rather abrupt change in the cyclic force-deformation response. Generally, members exhibit a very gradual deterioration of peak resistance with cycling and failure can be defined only conventionally (as the 15% drop in post-ultimate resistance).

So, on the envelope curves of each cross-section**,** the deformation at yielding, θ_y, and the ultimate deformation capacity, θ_u, corresponding to a lateral force response equal to 85% of the maximum, were measured. To this purpose, a straight line was drawn at the $0.85V_{max}$ level, intersecting the envelope at two points, one on the ascending and the other on the falling branch, as shown in Fig. (**8**). The rotation at yielding, θ_y, was the deformation determined by the point on the ascending branch and the rotation at ultimate, θ_u, was the deformation determined by the point on the falling branch of the envelope curve. The rotations of plastic hinges at yielding, θ_y and ultimate, θ_u, for the R/C members of infilled frames at critical sections are presented in Table **3**. It can be seen from these experimental results that failure of frames was governed by development of plastic hinges at the top and the bottom of the columns. Plastic hinges in all beams of infilled frames did not develop at all. Generally the infills restrained the beams from bending and therefore postponed the development of plastic hinges rotation at ultimate, θ_u, in the beams. On the other hand some very low values for rotation at yielding, θ_y, have been determined. This may be attributed to the local effects of infills too. In the case of the present investigation, the shear failure of the columns was not observed, as it was expected in design, because the infill was weak in relation to the reinforced concrete frames. It must be pointed out that the rotation at yielding, θ_y, will not necessarily coincide with the first yield of tensile reinforcement, which generally occurs at a somewhat lower rotation, particularly if the reinforcement is distributed around the section

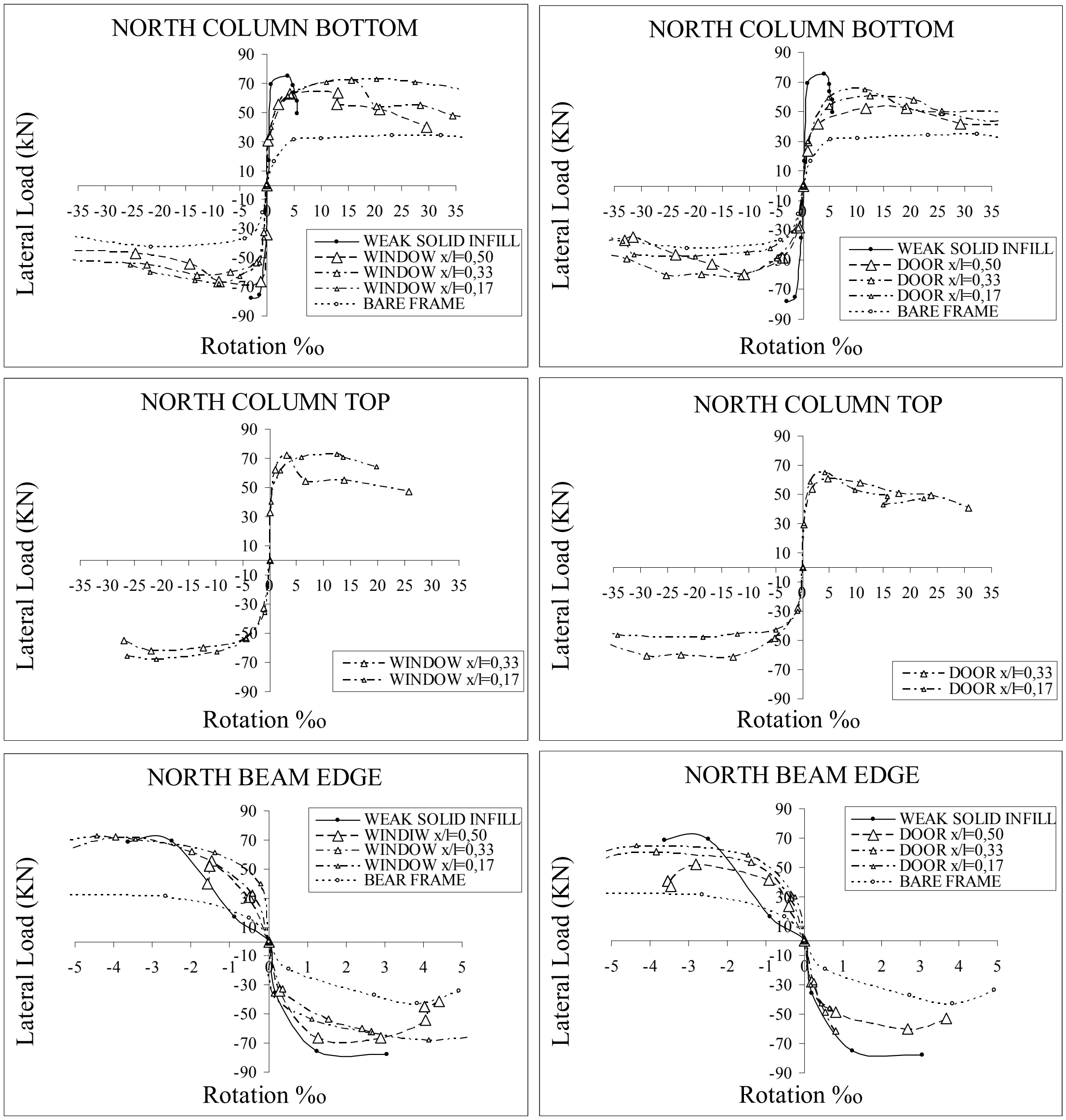

(a) **(b)**

Fig. (7). Lateral load-rotation envelopes: (**a**) window openings of various locations; and (**b**) door openings of various locations.

as would be the case for a column (Paulay and Priestley 1992) [21].

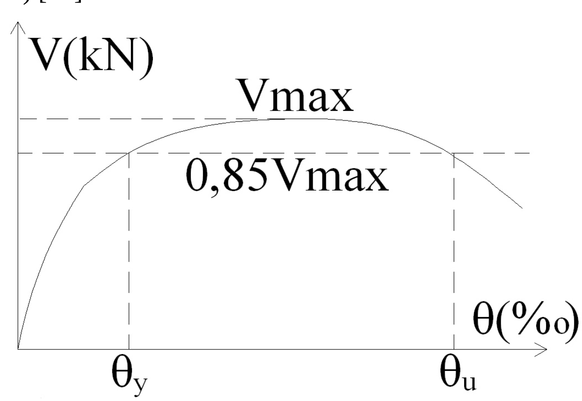

Fig. (8). Determination of rotation at yielding, θ_y and ultimate, θ_u, from the envelope curve.

DISCUSSION OF EXPERIMENTAL RESULTS

Influence of the Parameters of the Experimental Investigation

Comparing in Table **4** plastic rotation angles, θ_p, demonstrated by the experimental evidence, for columns of infilled frames, with the plastic rotation angles, θ_p, of bare frame, one observes that values for infilled frames are lower from values obtained for bare frame, by an average factor of: 0.70, 0.80 or 0.80 for weak infills with central openings, weak infills with eccentric openings or strong infills with central openings, respectively. The reason for the difference is that the lower experimental value expresses the effects of the infills on the columns, that are more pronounced in the case of weak infills with central openings. Infills with eccentric openings or strong infills with central openings exhibited a better performance. The above observations are compatible with those discussed from a mechanical standpoint by Kakaletsis and Karayannis 2007, 2008, and 2009 [14-16].

Table 3. Rotation at Yielding, θ_y and Rotation at Ultimate, θ_u, of R/C Members of Infilled Frames at Critical Sections

Specimen	Column bottom	Column top	Beam edge
	Rotation of plastic hinge at yielding, θ_y (‰)		
B	7,98/-5,18	6,44/-3,92	5,35/-5,01
S	0,7/-1,2	- -/- -	1,44/-1,13
WO2	1,7/-1	- - / - -	1,15/-1,08
WO3	0,5/-1,58	3,8/-1,38	0,28/-0,61
WO4	1,5/-0,49	2/-0,2	0,5/-0,21
DO2	5,5/-5,25	5,2/-2,63	0,91/-1,08
DO3	3,1/-3,1	3,6/-0,56	0,63/-1
DO4	3,6/-5,07	0,91/-4,61	1,51/-1,03
WX1*	4,4/-2,1	2/-5,62	1,38/-1,09
WX2*	5/-1,67	1,1/-3,8	2/-1,44
DX1*	4,35/-5,3	0,94/-4	- - /-0,7
DX2*	4,86/-6,33	1,79/-2	0,63/-1,18
IS	0/-3,3	3,6/-2	0,98/-0,86
IWO2	0/-1,6	2,4/-0,9	0,47/-0,3
IDO2	1,4/-1,4	2/-0,2	0,63/-0,26
	Rotation of plastic hinge at ultimate, θ_u (‰)		
B	34,16/0	26,6/-14,56	(N)/- (N)
S	5,1/-7,5	- / -	4,76/- (N)
WO2	11/-25,52	- / -	1,46/-4,2 (N)
WO3	5,8/-21,68	23,73/-17	- - /-2,9 (N)
WO4	- / -	- / -	- - /-4,33 (N)
DO2	21,84/-22,62	19,5/-17,11	3,08/-4,54 (N)
DO3	24,77/-23,73	24,58/-21,23	0,93/-1,96 (N)
DO4	32,85/ -	10/-19,28	2,87/-3,7 (N)
WX1*	40/-25,21	20,7/-26,7	10/-10,56 (N)
WX2*	18,42/-36,9	5,44/-29,3	2,55/-7,98 (N)
DX1*	17,52/-32,93	9/-40	- - / - (N)
DX2*	25/-31,81	17,24/-36,8	- - /-5,31 (N)
IS	7,4/-30,2	16,5/-30,2	4,56/-4,58 (N)
IWO2	5,6/-20,1	26/-17,8	1,54/0 (N)
IDO2	24,9/-25,7	13,4/0	1,61/0 (N)

*Instrumentation on the north joints (the rest of specimens instrumentation on the south joints).
N: Not happened.
- -: No data.

Comparison of the Determined Rotations

FEMA 356 [3] guidelines states that calculated component deformations are not permitted to exceed deformation limits for appropriate performance levels. Test data used in the present investigation are consistent with the descriptions of anticipated damage at structural performance level of "Structural stability", since the final horizontal offset approaches 40‰ interstory drift (ATC 40) [4]. For beams and columns, acceptance criteria are expressed in terms of plastic rotation angles within the yielding plastic hinge θ_p, as a function of flexural, shear, and splice actions in columns, with conforming and nonconforming transverse reinforcement. These guidelines give values for rotation at yielding, θ_y, in the end of the elastic range, at structural performance level of "Immediate occupancy", equal to 0.005 rads for RC beams and columns. Plastic hinges rotation at ultimate, θ_u, is derived as the sum $\theta_u = \theta_y + \theta_p$. This is approximately equal to the chord rotation or drift of the shear span (δ/L, where δ is the deflection at the member end and L is the member length). For the specimen of the present study, beams and columns are of "primary component type", "controlled by flexure", having "conforming reinforcement". Thus, plastic hinge rotation capacity is given as θ_p =0.020 and $\theta_u = \theta_y + \theta_p$=0.025.

The outcome of Table **3**, for plastic rotation angles, θ_p, for the column of bare pilot frame has been compared to the

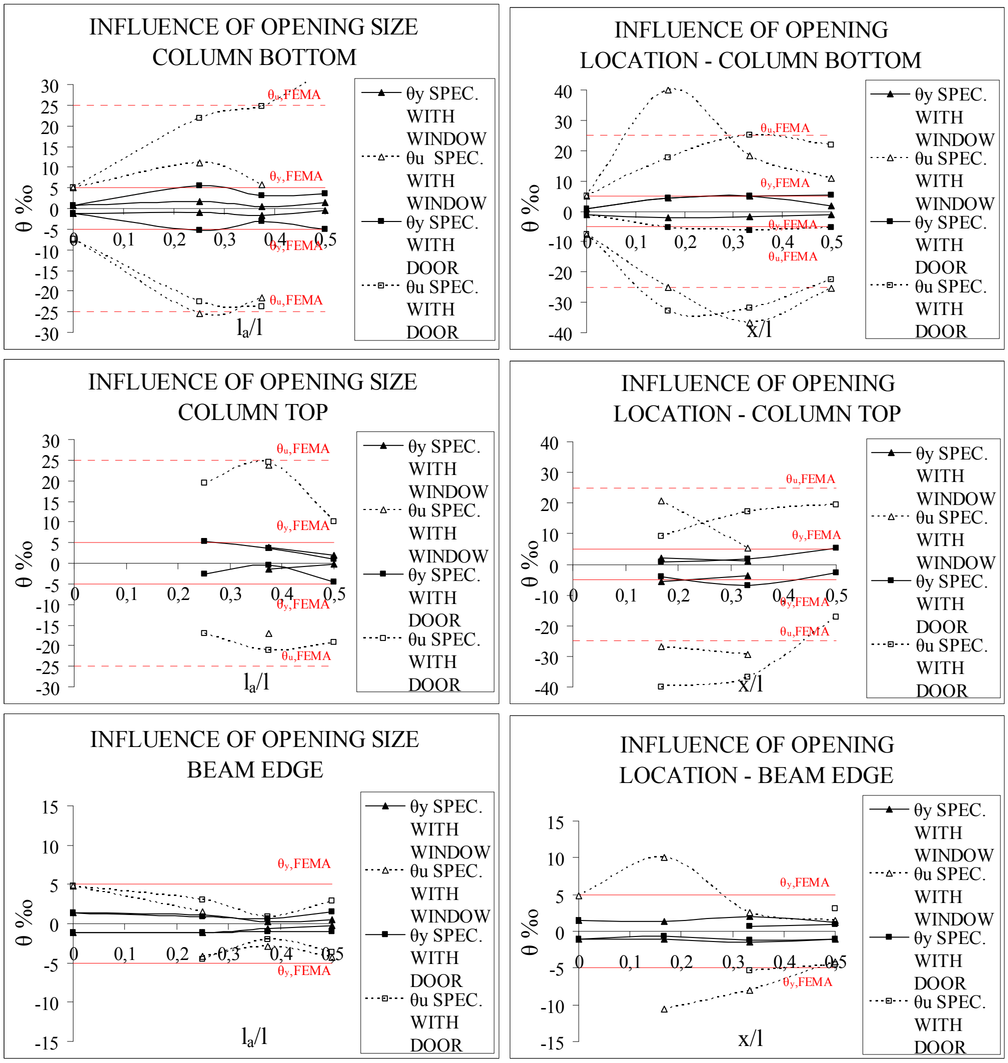

(a) Opening size **(b)** Opening location

Fig. (9). Rotation at yielding, θ_y and ultimate, θ_u, against (**a**) window and door central opening sizes and (**b**) window and door opening locations.

plastic rotation angle estimated in FEMA 356 [3]. The experimental plastic rotation exceeds the prediction of FEMA 356 [3] by an average factor of 1.1. So, values obtained from FEMA 356 [3] against values in the present study, for bare frame, are conservative, as expected.

Rotation at yielding, θ_y and ultimate, θ_u, against the parameters investigated for infilled frames are presented in Fig. (**9**) and Fig. (**10**).

Comparing in Table **4** plastic rotation angles, θ_p, for columns of infilled frames demonstrated by the experimental evidence, with the deformation limits of FEMA 356 [3], one observes that values in the present study are lower from values obtained from FEMA 356 [3], by an average factor of: 0.75, 0.90 or 0.90 for weak infills with central openings, weak infills with eccentric openings or strong infills with central openings, respectively. The reason for the difference is that the lower experimental value expresses the effects of the infills on the columns, that are more pronounced in the case of weak infills with central openings. Infills with eccentric openings or strong infills with central openings exhibited a better performance. The above observations are compatible with those discussed from a mechanical point of view by Kakaletsis and Karayannis 2007, 2008, and 2009 [14-16]. These effects are not taken into account in FEMA 356 [3] provisions.

CONCLUSIONS

The influence of masonry infills with openings on the rotations of R/C members of infilled frames at yielding and ultimate, under seismic loading was experimentally investigated vs the window and door opening width, the window and door opening location and the masonry strength.

The experimental results indicate that infills restrained the beams from bending and, consequently excluded the development of plastic hinges in the beams.

However, the presence, behavior and failure of the infills even in the cases with openings can significantly adversely

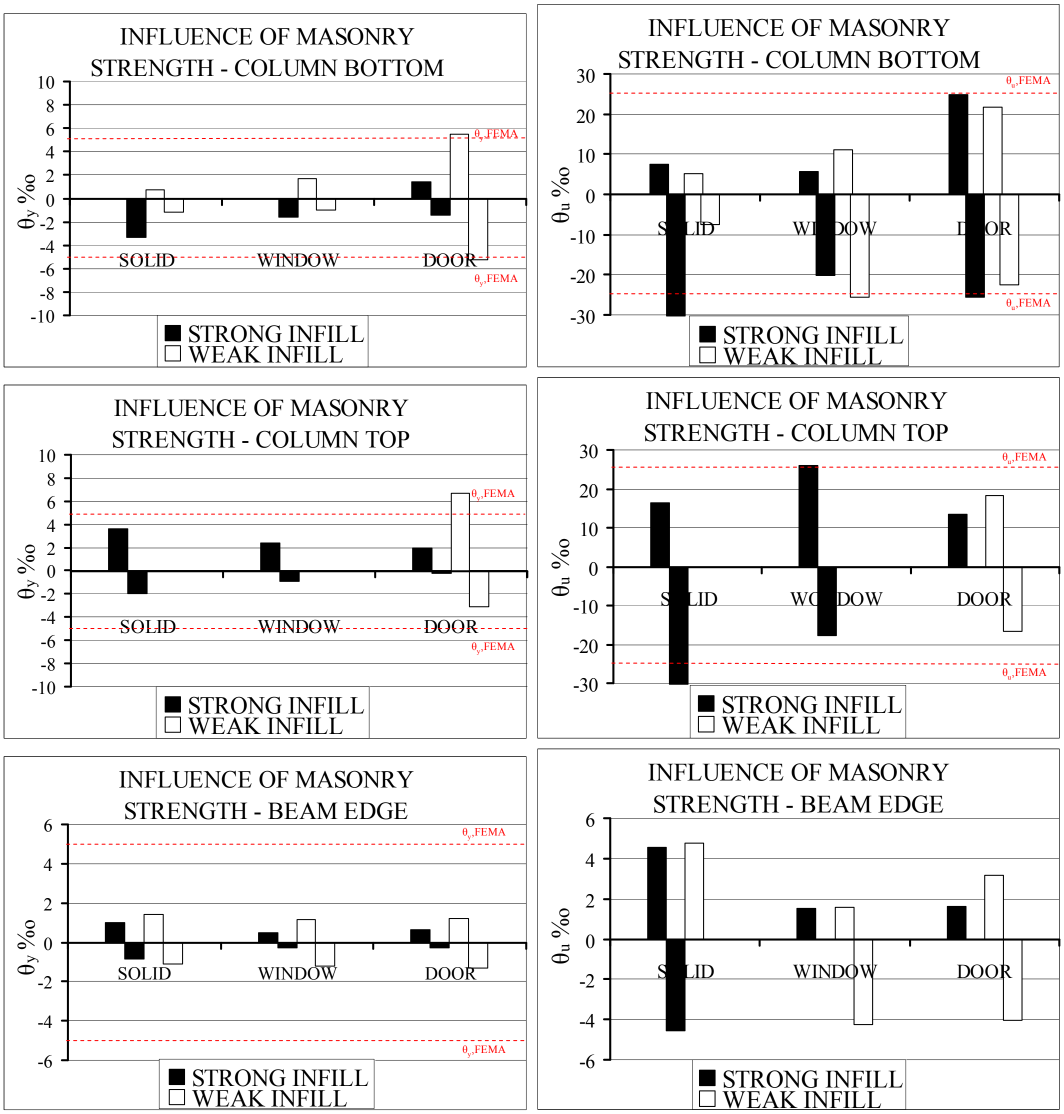

(a) Yielding, θ_y **(b)** Ultimate, θ_u

Fig. (10). Rotation (**a**) at yielding, θ_y and (**b**) at ultimate, θ_u, against infill strength.

Table 4. Comparison of Plastic Rotation Angles, θ_p, for Columns of Infilled Frames with those of: (a) Bare Frame; and (b): FEMA 356, as a Function of the Parameters Investigated

Opening Shape	Central Opening Size la/l	Plastic Rotation Ratios $\theta_p / \theta_{p,B}$ (at Column base / at Column top)	Plastic Rotation Ratios $\theta_p / \theta_{p,FEMA}$ (at Column base / at Column top)
Window	0	-/0.2	-/0.3
	0.25	-/0.6	-/0.8
	0.38	1.2/0.5	1/0.7
	0.5	-/-	-/-
	M.V.	**0.6**	**0.7**
Door	0	-/0.2	-/0.3
	0.25	0.9/0.6	0.7/0.8
	0.38	1.4/0.8	1.1/1.1
	0.5	0.8/1	0.6/1.4
	M.V.	**0.8**	**0.8**

Table 4. Contd….

Opening Shape	Opening Location x/l	Plastic Rotation Ratios θ_p / $\theta_{p,B}$ (at Column base / at Column top)	Plastic Rotation Ratios θ_p / $\theta_{p,FEMA}$ (at Column Base / at Column top)
Window	0	-/0.2	-/0.3
	0.17	1.3/1.1	1 /1.5
	0.33	1/0.9	0.8/1.3
	0.5	-/0.6	-/0.8
	M.V.	**0.8**	**0.9**
Door	0	-/0.2	-/0.3
	0.17	1.4/0.7	1.1/1
	0.33	1.6/0.8	1.3/1.1
	0.5	0.9/0.6	0.7/0.8
	M.V.	**0.8**	**0.9**

Infill strength	Opening Shape	Plastic Rotation ratios θ_p / $\theta_{p,B}$ (at Column Base / at Column top)	Plastic Rotation Ratios θ_p / $\theta_{p,FEMA}$ (at Column Base / at Column top)
Strong infills	Solid	-/0.6	-/0.8
	Window	1.3/0.4	1/0.6
	Door	0.8/0.9	0.6/1.3
	M.V.	**0.8**	**0.9**

-: No data.

affect the performance of R/C frames in terms of column deformations.

The location of the opening as close to the edge of the infill as possible provides an improvement to the performance of the columns of infilled frame.

The use of infill with improved compressive strength but almost identical shear strength decreases the adverse influence of the openings in terms of column deformations.

The factor of 0.75, 0.90 or 0.90 should be applied as correction factor, to the value of θ_p for columns, obtained from FEMA 356 [3] for weak infills with central openings, weak infills with eccentric openings or strong infills with central openings, respectively.

Nevetheless, taking into account all the involved uncertainties, the scale effects and the inadequate number of samples for each specimen, it has to be emphasized that the experimental results of the presented work and the above yielded conclusions are mainly limited to the study cases and must be used and extrapolated carefully and cautiously. It is recommended that more refined experimental techniques be pursued in future research.

CONFLICT OF INTEREST

The author confirm that this article content has no conflicts of interest.

ACKNOWLEDGEMENTS

The author is grateful to the Research Committee of Technological Educational Institution of Serres for the financial support of this research project.

REFERENCES

[1] ATC, "*NEHRP Guidelines for the Seismic Rehabilitation of Buildings*", FEMA Report 273, Washington, D.C: Applied Technology Council for the Building Seismic Safety Council, 1997.

[2] ATC, "*NEHRP Commentary on the Guidelines for the the Seismic Rehabilitation of Buildings*", FEMA Report 274, Washington, D.C: Applied Technology Council for the Buildings Seismic Safety Council, 1997.

[3] ASCE, *FEMA 356 Prestandard and Commentary for the Seismic Rehabilitation of Buildings*, Washington, D.C: ASCE for the Federal Emergency Management Agency, Nov. 2000.

[4] ATC 40, *Seismic Evaluation and Retrofit of Concrete Buildings*, vol 1, California: Applied Technology Council, November, 1996.

[5] Comite Euro international du Beton, *Ductility of Reinforced Concrete Structures*, *Bulletin d'Information* 242, T. Telford Ltd: London, May 1998.

[6] Comite Euro international du Beton, *Ductility-Reinforcement*, *Bulletin d'Information 218*, Beton, Lausanne: Aug. 1993.

[7] T.B. Panagiotakos, M.N. Fardis, "Deformations of RC members of infilled frames at yielding and ultimate," *ACI Struct. J.*, vol. 98, no. 2, pp. 135-148, 2001.

[8] M. N. Fardis, T. B. Panagiotakos, "Seismic design and response of bare and masonry-infilled reinforced concrete buildings. Part II: Infilledstructures," *J. Earthquake Eng.*, vol. 1, no. 3, pp. 475-503, 1997.

[9] M. N. Fardis, "Design provisions for masonry – infilled RC frames," In: *Proceedings of 12th World Conference on Earthquake Engineering*, p. 2553, 2000.

[10] M. N. Fardis, *Seismic Design, Assessment and Retrofitting of Concrete Buildings, based on EN-Eurocode 8, Series: Geotechnical, Geological, and Earthquake Engineering*, Springer: New York, 2009.

[11] H. A. Moghaddam, P. J. Dowling, "*The State of the Art in Infilled Frames"*, ESEE Research Report No, 87-2, London: Civil Engineering Department, Imperial College, pp. 231-284, 1987.

[12] CEB Comite Euro-International du Beton, *RC Frames under Earthquake Loading – State of the art report. Chapter 5: Reinforced Concrete Infilled frames*, London: Thomas Telford, pp. 231-303, 1996.

[13] G. Montal, S. K. Jain, "Lateral stiffness of masonry infilled reinforced concrete frames with central opening", *Earthquake Spectra*, vol. 24, no 3, pp. 701-723, 2008.

[14] D. J. Kakaletsis, C. G. Karayannis, "Experimental investigation of infilled R/C frames with eccentric openings", *Struct. Eng. Mech.*, vol. 26, no. 3, pp. 231-250, 2007.

[15] D. J. Kakaletsis, C. G. Karayannis, "Influence of masonry strength and openings on infilled R/C frames under cycling loading", *J. Earthquake Eng.*, vol. 12, no. 2, pp. 197-221, 2008.

[16] D. J. Kakaletsis, C. G. Karayannis, "Experimental investigation of infilled R/C frames with concentric openings", *ACI Struct. J.*, vol. 106, no. 2, pp.132-141, 2009.

[17] CEN European Standard EN 1998-1, Eurocode 8: Design of structures for earthquake resistance, Part 1: General rules, seismic actions and rules for buildings, Brusells: Comite European de Normalisation, 2004.

[18] CEN EUROPEAN STANDARD EN 998-2, *SPECIFICATION FOR MORTAR FOR MASONRY*, BRUSSELS: EUROPEAN COMMITTEE FOR STANDARDIZATION, PP. 1-17, 2001.

[19] H. Sezen, "*Seismic Behavior and Modeling of Reinforced Concrete Building Columns*", PhD thesis, University of California, Berkeley, 2002.

[20] K. J. Elwood, M. O. Eberhard, "Effective Stiffness of Reinforced Concrete Columns", *ACI Struct. J.*, vol. 106, no. 4, pp. 476-484, 2009.

[21] T. Paulay, M.J.N. Priestley, *Seismic Design of Reinforced Concrete and Masonry Buildings*, John Wiley & Sons: New York, vol. 142, 1992.

Received: November 28, 2011 Revised: April 28, 2012 Accepted: April 30, 2012